The 2016 World Congress on
The 2016 Structures Congress (Structures16)
Jeju Island, Korea, August 28-September 1, 2016

Ultimate strength of high-strength composite columns after sustained service loading

*Chang-Soo Kim[1], Hong-Gun Park[2], In-Rak Choi[3], and Kyung-Soo Chung[4]

[1] *School of Civil Engineering, Shandong Jianzhu Univ., Jinan, 250-101, China*
[2] *Dept. of Architecture and Architectural Eng., Seoul National Univ., Seoul, 151-742, Korea*
[3], [4] *POSCO Steel Solution Center, Incheon, 406-840, Korea*
[1] *mukan05@snu.ac.kr*

ABSTRACT

To investigate the ultimate strength of high-strength composite columns after sustained service loading, a numerical study was performed by time-dependent numerical analysis. For the analysis, the age-adjusted effective modulus method and relaxation solution procedure were used. The numerical analysis results generally agreed with test results, and the numerical parametric study showed that the long-term effect on the ultimate strength is not significant due to the low creep and shrinkage of high-strength concrete and the high internal restraint of high-strength steel. The design factors in current design codes for the long-term effective flexural stiffness relatively gave good predictions.

1. INTRODUCTION

The deformation of a steel-concrete composite column gradually increases with time due to the creep and shrinkage of concrete, and the long-term deformation may cause detrimental effects on the serviceability and ultimate strength of the column, such as the premature steel yielding and creep buckling (Gilbert 1988). Numerous experimental and numerical studies have been performed for the long-term behavior of composite columns, and generally, it is known that the long-term deformation results in reduction of the ultimate strength (Bridge 1979; Uy 2001; Han et al. 2004; and Ma and Wang 2012). However, some of existing studies showed different results: the long-term deformation has no significant effect on the ultimate strength (Löfgren et al. 1997; Chicoine et al. 2003; Kawano et al. 1998; and Chen and Dai 2015), or even increases the ultimate strength (Chacón et al. 2007; and Wang et al. 2011). Especially, the

[1] Associate Professor
[2] Professor
[3] Senior Researcher, PhD
[4] Principal Researcher, PhD

majority of the existing studies were limited to normal-strength materials and concentric loading. Thus, further studies are required on the effect of high-strength materials and eccentric loading.

2. TIME-DEPENDENT NUMERICAL ANALYSIS

To investigate the long-term effect on the structural behavior of composite columns, time-dependent numerical analysis was performed using the age-adjusted effective modulus method (Bazant 1972) and relaxation solution procedure (Bresler and Selna 1964; Gilbert 1988; Bradford and Gilbert 1990; Adrian and Triantafillou 1992; and Morino et al. 1996). To predict the creep coefficient $\phi_{cr}(t)$ and shrinkage strain $\varepsilon_{sh}(t)$ of concrete, the modified ACI 209R-92 model (ACI 1997; and Huo et al. 2001) was used [Eq. (1)]. In the modified model, the characteristics of high-strength concrete were taken into account: higher development of creep and shrinkage at early ages; and lower values of ultimate creep and shrinkage.

$$\phi_{cr}(t)=\frac{(t-t_0)^{0.6}}{K_{cr}+(t-t_0)^{0.6}}\phi_{cru}\left(\gamma_{cr,t0}\cdot\gamma_{cr,RH}\cdot\gamma_{cr,vs}\cdot\gamma_{cr,s}\cdot\gamma_{cr,\psi}\cdot\gamma_{cr,\alpha}\cdot\gamma_{cr,fc}\right) \quad (1a)$$

$$\varepsilon_{sh}(t)=\frac{(t-t_c)}{K_{sh}+(t-t_c)}\varepsilon_{shu}\left(\gamma_{sh,tc}\cdot\gamma_{sh,RH}\cdot\gamma_{sh,vs}\cdot\gamma_{sh,s}\cdot\gamma_{sh,\psi}\cdot\gamma_{sh,c}\cdot\gamma_{sh,\alpha}\cdot\gamma_{sh,fc}\right) \quad (1b)$$

where t = time, t_0 = loading age, and t_c = initial moist curing duration. ϕ_{cru} = ultimate creep coefficient, and ε_{shu} = ultimate shrinkage strain. $\gamma_{cr,t0}$, $\gamma_{cr,RH}$, $\gamma_{cr,vs}$, $\gamma_{cr,s}$, $\gamma_{cr,\psi}$, $\gamma_{cr,\alpha}$, $\gamma_{cr,fc}$ = creep correction factors for loading age (t_0), ambient relative humidity (RH), volume-to-surface ratio (v/s), slump (s), fine aggregate ratio (ψ), air content (α), and concrete strength (= 1.18 – 0.0065f_c'), respectively. $\gamma_{sh,tc}$, $\gamma_{sh,RH}$, $\gamma_{sh,vs}$, $\gamma_{sh,s}$, $\gamma_{sh,\psi}$, $\gamma_{sh,c}$, $\gamma_{sh,\alpha}$, $\gamma_{sh,fc}$ = shrinkage correction factors for initial moist curing duration (t_c), ambient relative humidity, volume-to-surface ratio, slump, fine aggregate ratio, cement content (c), air content, and concrete strength (= 1.20 – 0.0073f_c'), respectively. K_{cr}, K_{sh} = adjustment factors for early-age creep (= 12 – 0.0725f_c') and shrinkage (= 45 – 0.3626f_c').

For the numerical analysis, a fiber model method was used considering the strain-compatibility and the confinement effect of the steel section and transverse bars (Kim et al. 2012 and 2014). The full analysis procedure consisted of three steps: 1) long-term loading on the composite column; 2) analysis of the long-term response; and 3) analysis of the ultimate load capacity after long-term loading.

For verification, the results of the time-dependent numerical analysis were compared with those of a previous experimental study. In the previous experimental study, ultimate load tests were performed after long-term load tests for three concrete-encased steel (CES) columns (C1, C2, and C3) and a concrete-filled steel tube (CFT) column (C4). Table 1 summarizes the properties of the test specimens. By using the measured values of ϕ_{cru} = 1.44, ε_{shu} = 553, and ε_{asu} = 161 (ultimate autogenous shrinkage strain) from the long-term load tests, the time-dependent numerical analysis was performed. Figs. 1 and 2 show the comparisons of the numerical analysis results with the long-term load test results and ultimate load test results. As shown in the figures, although there was some discrepancy in the long-term behavior, the numerical analysis results (thin lines) generally agreed with the test results (thick solid lines). At t = 147 days, the mean value and standard deviation of the ratios of the numerical analysis result to the test result were 92% and 0.113 for long-term strains, 96% and 0.038 for internal forces, or 107% and 0.037 for peak loads, respectively.

Table 1 Properties of Test Specimens

Specimens		CES			CFT
		C1	C2	C3	C4
Section	Dimensions, $B \times D$ (mm)	180×180	180×180	180×180	180×180
	Gross Area, $A_g = BD$ (mm^2)	32400	32400	32400	32400
Concrete	$f'_{c.28}$ (MPa)	104	104	104	104
Steel	f_{ys} (f_{us}, MPa)	812 (868)	812 (868)	812 (868)	812 (868)
	Steel Shape (b_s/t_s)	H-80×80×15×15 (2.17)	H-80×80×15×15 (2.17)	H-80×80×15×15 (2.17)	□-80×80×15 (10)
	Steel Ratio, $\rho_s = A_s/A_g$ (%)	9.7	9.7	9.7	30.6
Longitudinal Bars	No. and Dia. (f_{yl}, MPa)	4-D10 (474)	4-D10 (474)	4-D10 (474)	-
	Rebar Ratio, $\rho_{sl} = A_l/A_g$ (%)	0.9	0.9	0.9	-
Overall Compressive Strength	Composite Section, P_0 (kN)*	5243.7	5243.7	5243.7	10020.2
	Steel Contribution, P_s/P_0	0.49	0.49	0.49	0.80
Net Column Length, L (mm) (Total Specimen Length, L_k)		980 (980)	980 (2140)	980 (2880)	980 (2880)
Slenderness Ratio, $\lambda = KL_k/r$**		26.1	58.1	76.7	43.7
Transverse Bars	Arrangement (f_{yt}, MPa)	D6@90mm (348)	D6@90mm (348)	D6@90mm (348)	-
	Vol. Ratio, ρ_t	0.98	0.98	0.98	-
Eccentricity of Axial Load, e_0 (mm) (Eccentricity, e_0/D)		0 (0)	0 (0)	30 (0.167)	30 (0.167)
Long-term Load, P_{LT}***		-	$0.4P_u$	$0.4P_u$	$0.4P_u$

* $P_0 = 0.85 f_c' A_c + f_{ys} A_s + f_{yl} A_l$

** Effective length factor K = 1, Radius of gyration $r = \sqrt{(0.2E_cI_c + E_sI_s)/(0.2E_cA_c + E_sA_s)}$ (mm, ACI 318-14), $E_c = 3320\sqrt{f_c'} + 6900$ (MPa, ACI 363R), and E_s = 205 GPa.

*** P_u = Short-term ultimate strength predicted by numerical analysis

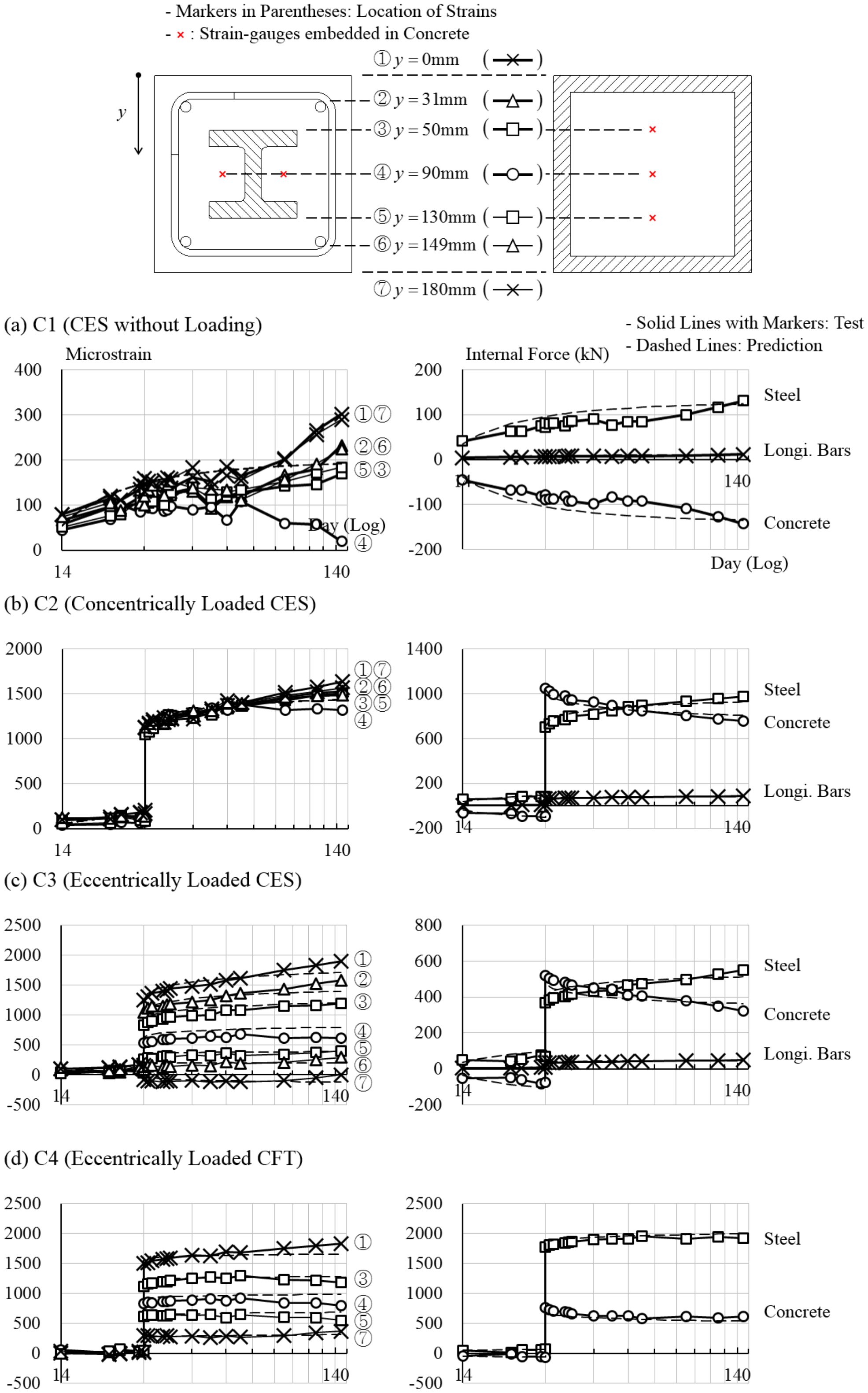

Fig. 1 Strains and Internal Forces of Composite Columns

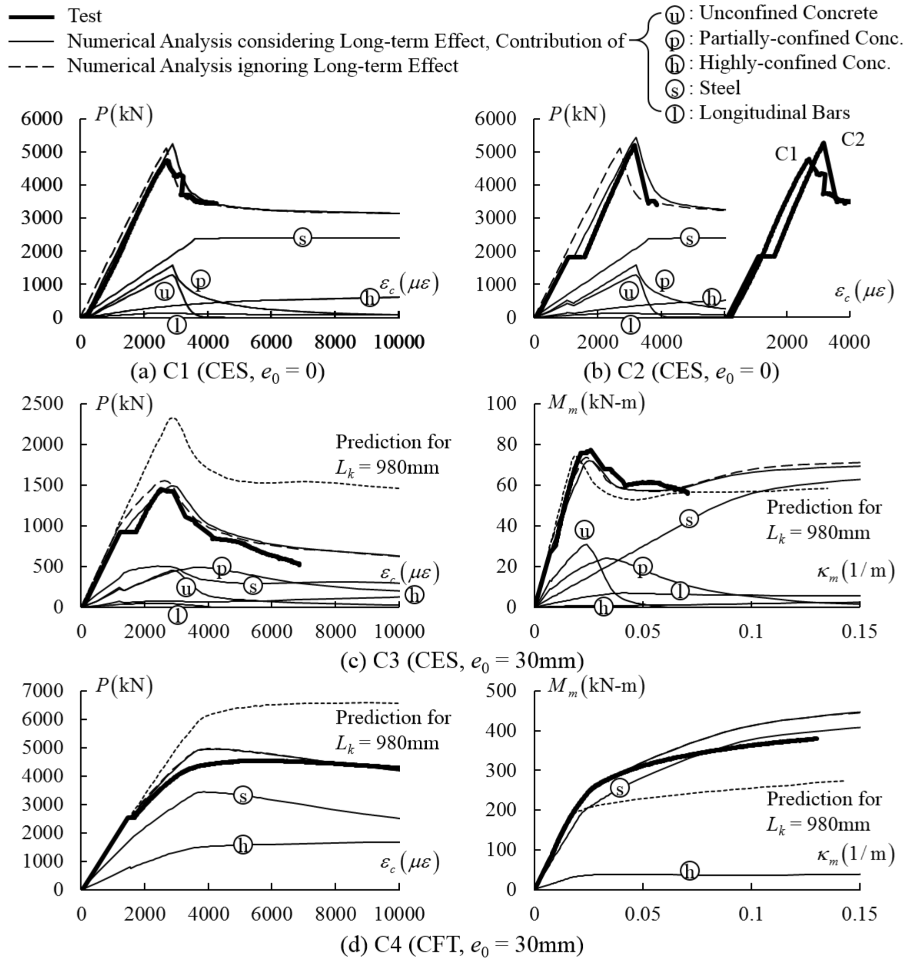

Fig. 2 Axial Load – Strain and Moment – Curvature Relationships at Mid-height Section

For detailed investigation, the strength contributions of the unconfined concrete (cover concrete), partially-confined concrete (confined by transverse bars), highly-confined concrete (confined by transverse bars and steel), steel, and longitudinal bars obtained from the numerical analysis are separately shown in Fig. 2 (thin solid lines with markers), and the numerical analysis results ignoring the long-term effect are also shown in the figure (thin dashed lines). The long-term effect decreased the strength contribution of the concrete and increased that of the steel and longitudinal bars. In the case of the concentrically loaded columns C1 and C2, the long-term effect increased the axial strength by 2% for C1 and 6% for C2 (by comparing the numerical analysis results with and without long-term loading). This is because the long-term effect induced the stress redistribution from the concrete to the high-strength steel in the composite section, in which the ultimate strength was determined by the crushing failure of the concrete prior to the yielding of the steel, and as a result, the steel stress at the concrete crushing was more increased, which resulted in increase of the ultimate strength. On the other hand, in the eccentrically loaded columns, the axial strength was decreased by 4% for C3 and 0.2% for C4 due to the additional 2nd-order effect caused by creep. Generally, in the high-strength composite columns, the long-term effect was less pronounced due to the dense matrix and low water-cement ratio of high-strength concrete and the high internal restraint of high-strength steel. Especially in the CFT column C4, the long-term effect was negligible due to the high steel ratio and fully sealed condition.

3. PARAMETRIC STUDY

Current design codes use the moment-magnification procedure to calculate the 2nd-order elastic moment of columns on the basis of the 1st-order elastic analysis result. The moment-magnification factor is affected by the effective flexural stiffness EI_{eff} of the column, and the long-term effect is considered in design by reducing the effective flexural stiffness [Eq. (2)].

$$EI_{eff} = \frac{0.2E_c I_g}{1+\beta_{dns}} + E_{ss}I_{ss} \text{ in ACI 318-14, where } \beta_{dns} = P_{LT}/P_u \quad (2a)$$

$$EI_{eff} = 0.9\left(E_{ss}I_{ss} + E_{sl}I_{sl} + 0.5E_{c,eff}I_c\right) \text{ in Eurocode 4, where } E_{c,eff} = E_c\frac{1}{1+\left(P_{LT}/P_u\right)\phi_{cr}} \quad (2b)$$

To investigate the effect of design parameters on the effective flexural stiffness, a numerical parametric study was performed for a prototype CES column shown in Fig. 3: cross-section = 700×700 mm; wide-flange = 300×200×t_s×t_s mm (t_s = variable thickness); longitudinal bars = 4-D25; and transverse bars = D13@175 mm. The parameters included the values of the ultimate creep coefficient and ultimate shrinkage strain [ϕ_{cru} = 1.30, 2.35, and 4.15 and ε_{shu} = 415, 780, and 1070 $\mu\varepsilon$ as specified in ACI 209R-92, before considering the correction factors of Eq. (1)], steel ratio ($\rho_s = A_s/A_g$ = 1, 2, and 4% or t = 7.2, 14.6, and 30.7 mm), steel strength (f_{ys} = 400, 600, and 800 MPa), concrete strength (f_c' = 30, 50, and 100 MPa), eccentricity ratio (e_0/D = 0.1, 0.3, and 1.0), and column length (L = 4, 6, and 8 m). To consider the extreme case in the specified range of ACI 209R-92, t_c = 1 day, t_0 = 7 days, RH = 40%, s = 70 mm, ψ = 50%, c = 446 kg/m^3, and α = 6% were assumed, and the long-term load P_{LT} = 0.4P_u and t = 10 years were used. From the parametric study results, the effective flexural stiffness of the composite column was evaluated by using Eq. (3)

$$EI_{eff} = \frac{PL^2}{4\left[\sec^{-1}\left(\frac{M_s}{M_c}\right)\right]^2} \text{ (Mirza and Tikka, 1999)} \quad (3)$$

where $M_s = P(e_0 + \Delta_m)$= moment at mid-height section, and $M_c = Pe_0$ = moment at column ends.

As shown in Fig. 3, the current design codes generally underestimated the effective flexural stiffness EI_{eff}. The short-term stiffness ratio $\alpha = EI_{eff}/E_cI_g$ (I_g = moment of inertia of gross section) evaluated from the numerical analysis varied with the design parameters, and was in the range of 0.14 – 0.94 [Fig. 3(a)]. On the other hand, α evaluated from the design codes, which neglect the effects of the design parameters, was relatively constant in the range of 0.22 – 0.27 for ACI 318-14 or 0.50 – 0.54 for Eurocode 4. Particularly, the design codes excessively underestimated EI_{eff} in the case 13 [e_0/D = 0.1 in Fig. 3(a)]. However, the design codes overestimated EI_{eff} in the case 15 [e_0/D = 1.0 in Fig. 3(a)], which may result in unsafe design. On the other hand, the simple factors in Eq. (2) for the long-term effect gave relatively good results: the ratio of the long-term stiffness to the short-term stiffness was $EI_{eff,L}/EI_{eff,s}$ = 0.92 for the time-dependent numerical analysis, 0.74 for ACI 318, or 0.76 for Eurocode 4 [Fig. 3(b)].

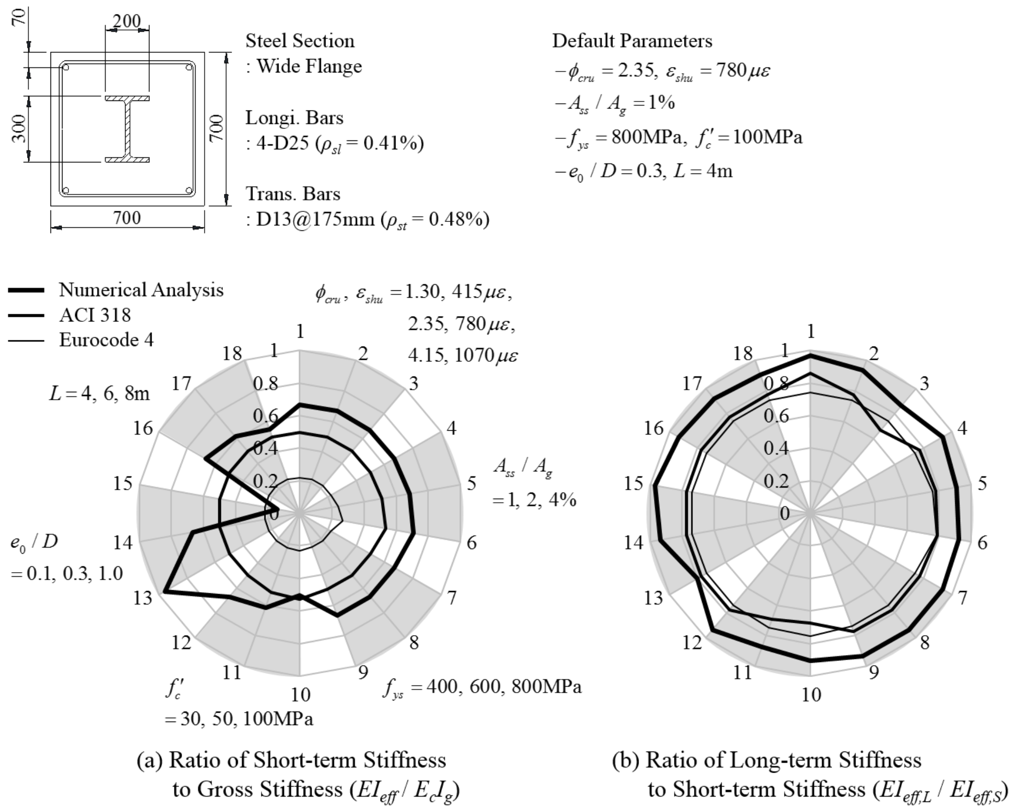

Fig. 3 Numerical Parametric Study for Effective Flexural Stiffness

3. CONCLUSIONS

To investigate the long-term effect on the structural behavior of composite columns, time-dependent numerical analysis was performed using the age-adjusted effective modulus method and relaxation solution procedure. The predictions by the numerical analysis were well matched with the long-term load test results and ultimate load test results. In the case of the concentrically loaded CES columns using high-strength steel, the long-term effect unexpectedly increased the ultimate strength. This is because the stress of the high-strength steel at the crushing failure of the concrete was increased by the long-term effect. On the other hand, in the eccentrically loaded columns, the effect of long-term loading on the ultimate strength was insignificant, because the stress increase of the high-strength steel by the long-term effect was offset by the 2nd-order effect. The parametric study showed that the current design codes did not give accurate predictions for the short-term effective flexural stiffness, but the design factors for the long-term effect relatively well predicted the ratio of the long-term stiffness to the short-term stiffness.

REFERENCES

Adrian, C.A., and Triantafillou, T.C. (1992), "Creep and shrinkage analysis of composite systems under axial load and biaxial bending," *Materials and Structures*, 25, 543-551.

ACI (American Concrete Institute). (1997), "Prediction of creep, shrinkage, and temperature effects in concrete structures," *ACI 209R-92*, Farmington Hills, MI.

ACI (American Concrete Institute). (2014), "Building code requirements for structural concrete and commentary," *ACI 318-14*, Farmington Hills. MI.

ACI (American Concrete Institute). (2010), "Report on high-strength concrete," *ACI 363R*, Farmington Hills. MI.

Bazant, Z.P. (1972), "Prediction of concrete creep effects using age-adjusted effective modulus method," *ACI Journal*, 69(4), 212-217.

Bradford, M.A., and Gilbert, R.I. (1990), "Time-dependent analysis and design of composite columns," *Journal of Structural Engineering, ASCE*, 116(12), 3338-3357.

Bresler, B., and Selna, L. (1964), "Analysis of time-dependent behaviour of reinforced concrete structures," *Proceedings of Symposium on Creep of Concrete, ACI Special Publication*, 9(5), 115-128.

Bridge, R.Q. (1979), "Composite columns under sustained load," *Journal of the Structural Division, ASCE*, 105(ST3), 563-576.

CEN (European Committee for Standardization). (2004), "Design of composite steel and concrete structures – Part 1-1: General rules and rules for buildings," *Eurocode 4*, Brussels.

Chacón, R., Mirambell, E., and Marí A. (2007), "Long-term response of concrete-encased composite columns," *Structures and Buildings*, 160(SB5), 273-285.

Chen, Z. and Dai, T. (2015), "Effects of sustained axial loads on steel-reinforced concrete columns," *HKIE Transactions*, 22(1), 16-22.

Chicoine, T., Massicotte, B., and Tremblay, R. (2003), "Long-term behavior and strength of partially encased composite columns made with built-up steel shapes," *Journal of Structural Engineering, ASCE*, 129(2), 141-150.

Gilbert, R.I. (1988), *Time Effects in Concrete Structures*, Elsevier Science Publishing Company Inc., NY.

Han, L.H., Tao, Z., and Liu, W. (2004), "Effects of sustained load on concrete-filled hollow structural steel columns," *Journal of Structural Engineering, ASCE*, 130(9), 1392-1404.

Huo, X.S., Al-Omaishi, N., and Tadros, M.K. (2001), “Creep, shrinkage, and modulus of elasticity of high-performance concrete,” *ACI Materials Journal*, 98(6), 440-449.

Kawano, A., Matsui, C., and Yukino, T. (1998), “Time-dependent effects on earthquake-resistant capacities of steel – concrete composite structures.” *Journal of Structural and Construction Engineering, Transactions of AIJ*, 508, 143-150. (in Japanese)

Kim, C.S., Park, H.G., Chung, K.S., and Choi, I.R. (2012), “Eccentric axial load testing for concrete-encased steel columns using 800 MPa steel and 100 MPa concrete,” *Journal of Structural Engineering, ASCE*, 138(8), 1019-1031.

Kim, C.S., Park, H.G., Chung, K.S., and Choi, I.R. (2014), “Eccentric axial load capacity of high-strength steel – concrete composite columns of various sectional shapes,” *Journal of Structural Engineering, ASCE*, 140(4), 04013091-1-12.

Löfgren, A.I., Kawano, A., and Warner, R.F. (1997), “Simplified design methods for slender composite columns under sustained and short term loads,” *Concrete 97 Conference, Concrete Institute of Australia*, 1-11.

Ma, Y., and Wang, Y. (2012), “Creep of high strength concrete filled steel tube columns,” *Thin-Walled Structures*, 53, 91-98.

Mirza, S.A., and Tikka, T.K. (1999), “Flexural stiffness of composite columns subjected to major axis bending,” *ACI Structural Journal*, 96(1), 19-28.

Morino, S., Kswanguchi, J., and Cao, Z.S. (1996), “Creep behavior of concrete-filled steel tubular members,” *Proceedings of an Engineering Foundation Conference on Steel – Concrete Composite Structure, ASCE*, 514-525.

Uy, B. (2001), “Static long-term effects in short concrete-filled steel box columns under sustained loading,” *ACI Structural Journal*, 98(1), 96-104.

Wang, Y., Geng, Y., Ranzi, G., and Zhang, S. (2001), “Time-dependent behaviour of expansive concrete-filled steel tubular columns,” *Journal of Constructional Steel Research*, 67, 471-483.